Catalysis Today 142 (2009) 52–60

Contents lists available at ScienceDirect

Catalysis Today

journal homepage: www.elsevier.com/locate/cattod

Preparation and characterization of Ru/MgO-Al_2O_3 catalysts for methane steam reforming

Luciene Santos Carvalho [a,b], André Rosa Martins [a], Patrício Reyes [c], Marcelo Oportus [c], Alberto Albonoz [d], Valéria Vicentini [e], Maria do Carmo Rangel [a,*]

[a] GECCAT, Instituto de Química, Universidade Federal da Bahia, Rua Barão de Geremoabo, s/n, Campus Universitário de Ondina, Federação, 40170-290 Salvador, Bahia, Brazil
[b] Departamento de Ensino, Centro Federal de Educação Tecnológica da Bahia, UE Camaçari, Av. Eixo Central, s/n, Centro, 42800 000 Camaçari, Bahia, Brazil
[c] Facultad de Ciencias Químicas, Universidad de Concepción, Casilla 3-C, Concepción, Chile
[d] Centro de Química, Instituto Venezolano de Investigaciones Científicas, 21827, Caracas, Venezuela
[e] Oxiteno S/A Indústria e Comércio, Avenida Ayrton Senna da Silva, 3001, 09380-440 Mauá, São Paulo, Brazil

ARTICLE INFO

Article history:
Available online 14 February 2009

Keywords:
Steam reforming
Hydrogen production
Ruthenium catalyst
Mg-Al oxide

ABSTRACT

The preparation and characterization of aluminum and magnesium oxides-supported ruthenium were described in this work, aiming to compare different supports to methane steam reforming catalysts for producing hydrogen. Gama-alumina-supported ruthenium and periclase-supported ruthenium were produced. The addition of small amounts of magnesium to alumina-supported ruthenium in the range of Mg/Al (molar) = 0.2–0.5 did not change the gama-alumina structure while high amounts (Mg/Al (molar) = 5) led to the production of periclase. Magnesium caused a decrease of specific surface area of alumina-supported ruthenium catalysts and this effect increased with the amount of the metal in solids. Magnesium also decreased the acidity of alumina-supported ruthenium and generated electron deficient ruthenium species, besides increasing their interaction with the support. The addition of magnesium increased the ruthenium dispersion but did not increase the methane conversion, suggesting that it negatively changed the electron properties of ruthenium towards methane conversion. However, it avoided deactivation during reaction and changed the activity for the water gas shift reaction, allowing tailoring the hydrogen to carbon monoxide molar ratio. The catalysts showed activity close or higher than a commercial sample, indicating that they are promising for the reaction, with the advantage that it can be tailored for several applications.

1. Introduction

Pure hydrogen has found several applications as fuel and as raw material for chemical and petrochemical industries. In the last years, it has been recognized as one of the most important fuels due to its potential applications in fuel cells for reducing environmental contamination and energy consumption [1]. Another fundamental feedstock for refining and petrochemical industries is the synthesis gas ($CO + H_2$), largely used in hydrotreating and hydrocracking processes as well as in methanol synthesis, gasoline production from methanol, ammonia synthesis and in hydrocarbon synthesis by Fischer–Tropsch process [2,3].

Although some processes such as dry reforming [4–6] and autothermal reforming [7,8] have been pointed out as promising for obtaining hydrogen and synthesis gas, the main commercial route is still the steam reforming. It is also the most economic and convenient process in regions where natural gas is available in large amounts [9,10]. In this case, a mixture of hydrogen, carbon monoxide and carbon dioxide is obtained from the reaction of light hydrocarbons (from natural gas or oil naphtha) and steam, over alumina-supported nickel catalysts, containing 10–25% nickel oxide [11]. The reaction, represented by Eq. (1), is strongly endothermic and then is often carried out at high temperatures (873–1173 K) and pressures ranging 20–40 bar [12]. In general, the steam reforming is followed by the water gas shift reaction (WGSR), which is slightly exothermic, as shown by Eq. (2) [13,14].

$$CH_{4(g)} + H_2O_{(g)} \rightleftarrows CO_{(g)} + 3H_{2(g)} \qquad \Delta H^\circ = 206.0\,\text{kJ mol}^{-1} \qquad (1)$$

$$CO_{(g)} + H_2O_{(g)} \rightleftarrows CO_{2(g)} + H_{2(g)} \qquad \Delta H^\circ = -41.2\,\text{kJ mol}^{-1} \qquad (2)$$

In order to get high methane conversions and to avoid coke deposition, by methane cracking (Eq. (3)) or by Boudouard reaction (Eq. (4)), the process is carried out under large amounts of steam

* Corresponding author. Tel.: +55 71 3283 6837; fax: +55 71 3235 5166.
E-mail address: mcarmov@ufba.br (M.d.C. Rangel).

0920-5861/$ – see front matter © 2009 Elsevier B.V. All rights reserved.
doi:10.1016/j.cattod.2009.01.010

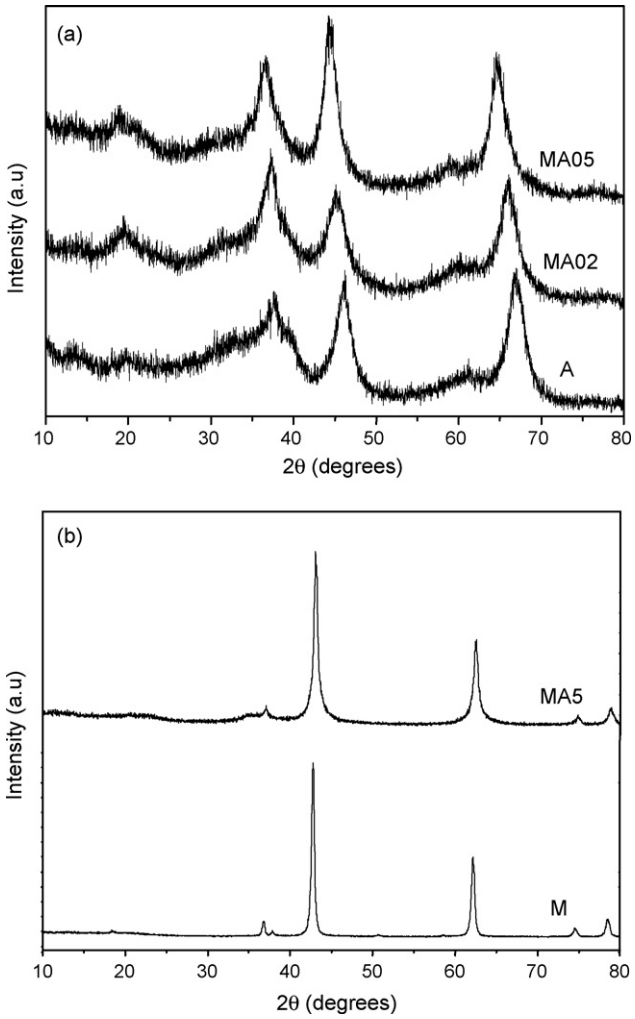

Fig. 1. X-ray diffractograms of (a) aluminum oxide (A) and aluminum and magnesium oxides with magnesium to aluminum molar ratio of 0.2 (MA02) and 0.5 (MA05) and of (b) magnesium oxide (M) and aluminum and magnesium oxide with magnesium to aluminum molar ratio of 5 (MA5).

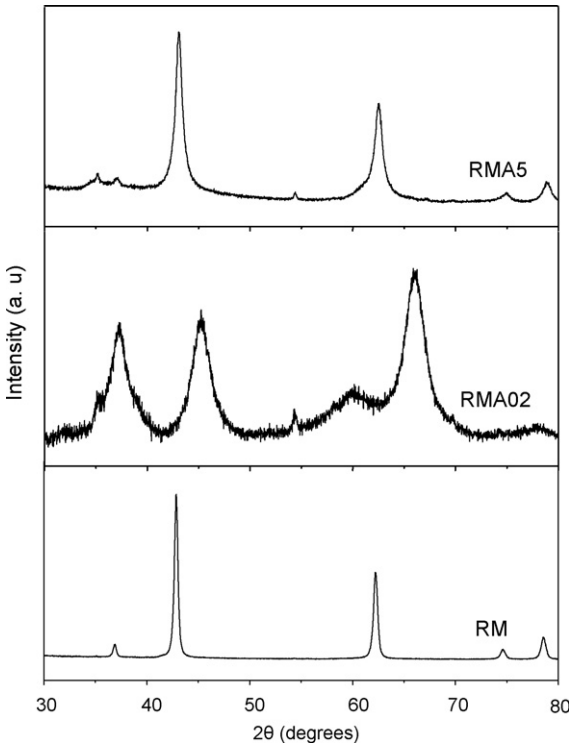

Fig. 2. X-ray diffractograms of magnesia-supported ruthenium (RM) and aluminum and magnesium oxides-supported ruthenium (RMA5 and RMA02). The numbers indicate the magnesium to aluminum molar ratio.

[11,12,15]. A high steam to carbon ratio shifts the equilibrium to favor the hydrogen production producing a hydrogen-rich gas. The industrial reformers work under steam to carbon molar ratios in the range of 2–5 [1,14].

$$CH_4 \rightleftarrows C + 2H_2 \qquad \Delta H^\circ = 75.0\,\text{kJ mol}^{-1} \tag{3}$$

$$2CO \rightleftarrows CO_2 + C \qquad \Delta H^\circ = 86.2\,\text{kJ mol}^{-1} \tag{4}$$

In spite of this fact, these operation conditions lead to the catalyst deactivation, generating a technological problem related to the commercial catalysts. Besides deactivation by coke, the support and the metal sinterization can also occur, resulting in a decrease of specific surface area. Therefore, the thermal stability of the catalyst is also a very important property to be considered [16], besides the high resistance against coke formation and the high mechanical resistance required for industrial applications [17]. These features are determined by the textural, structural and physical-chemistry properties of the catalysts, which can be tailored during solid preparation [18].

The support plays an important role in the control of the catalyst characteristics and its chemical and textural properties can also be tailored by the use of different combinations of metal oxides. The mixed oxides, for instance, have been pointed out as a new class of supports which, in several cases, can tailor the properties of the catalysts and then increase their activity and selectivity, as compared to the classical gama-alumina, largely used in the formulation of commercial steam reforming catalysts [19]. Alumina is an acidic support which can catalyze secondary reactions such as polymerization and cracking, leading to coke deposition on the catalyst surface and to the blockage of the active sites. Therefore, the mixed oxides with tailored properties can be good candidates to replace alumina for several applications.

On the other hand, noble metals such as platinum, ruthenium and iridium have been pointed out as a convenient option to overcome the problem of coke deactivation and then they are promising catalysts to steam reforming [20].

With the purpose of finding active and selective catalysts to produce hydrogen by methane steam reforming, which are able to prevent coke deposition, the preparation and characterization of aluminum and magnesium oxides-supported ruthenium were described in this work. In order to evaluate the effect of the content of magnesium oxide on their properties, catalysts with different magnesium to alumina molar ratios were obtained.

It is well known that the strength and concentration of aluminum acidic sites can be changed by various elements. For example, cations of the three first groups in periodic table have been used as dopants for alumina-based catalysts [21–23]. Among them, the magnesium-modified alumina is considered promising as catalyst and as support [24,25]. In order to neutralize the stronger acidic sites of alumina and find supports with lower acidity and higher thermal stability, magnesium oxide has been added to alumina in some formulations. The basic character of magnesium oxide as well as the high specific surface and the stability of alumina bring out a promising combination for application as support in steam reforming catalysts.

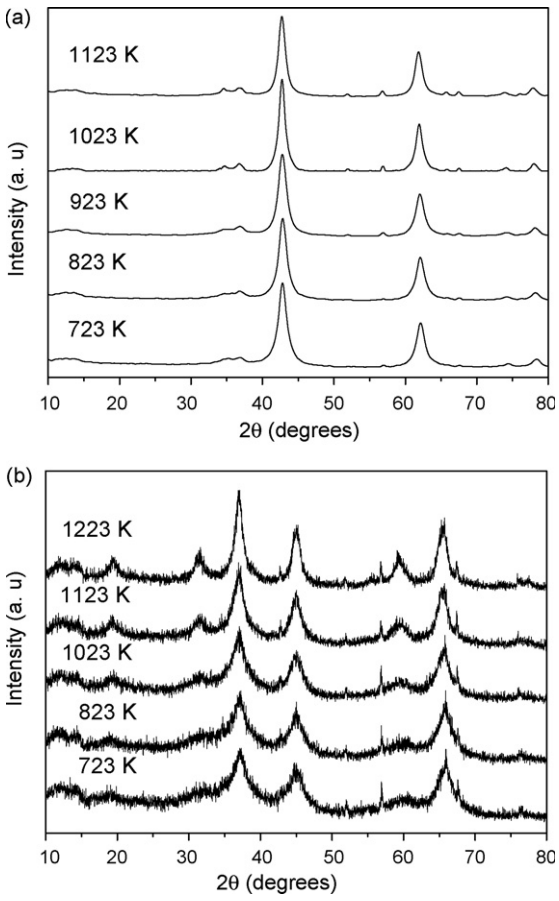

Fig. 3. X-ray diffractograms of aluminum and magnesium oxides-supported ruthenium with (a) Mg/Al = 5 (RM5 sample) and (b) Mg/Al = 0.2 (RMA02 sample) taken at different temperatures.

2. Experimental

2.1. Samples preparation

Supports were prepared by the hydrolysis of aluminum nitrate and magnesium nitrate with concentrated ammonium hydroxide solution at room temperature and pH 9. The as-obtained precipitate was maturated, centrifuged and washed with an ammonium hydroxide solution. The sample was dried at 393 K, for 24 h and calcined under air flow at 723 K, for 8 h. Solids with different magnesium to aluminum molar ratio were obtained: Mg/Al (molar) = 0.2 (MA02 sample), Mg/Al = 0.5 (MA05) and Mg/Al = 5 (MA5). Pure aluminum (A) and magnesium (M) oxides were also prepared using the same procedure.

All oxides were impregnated with ruthenium (III) chloride solution to obtain catalysts containing 1 wt.% of the metal (RA, RM, RMA02, RMA05 and RMA5 samples). After impregnation, the solids were dried at 393 K, for 12 h and calcined at 723 K, for 8 h. This low temperature was selected to prevent the hydrolysis of magnesium oxide which could occur at higher temperatures (above 723 K).

2.2. Samples characterization

The samples were characterized by X-ray diffraction (XRD), specific surface area (Sg) and porosity measurements, temperature programmed reduction (TPR), temperature programmed desorption (TPD) of ammonia, cyclohexane dehydrogenation, ruthenium dispersion measurements and X-ray photoelectronic spectroscopy.

X-ray diffractograms were obtained using a model Shimadzu XRD600 equipment with a nickel filter. The sample was exposed to CuKα radiation and then a scanning in the range of 2θ of 10–80° was carried out. The stability of the catalysts upon heating was monitored by getting X-ray diffractograms at different temperatures (723, 823, 923, 1023 and 1123 K), after heating the samples in situ in a chamber. The solids were heated at a rate of 10° min^{-1} under air flow (100 mL min^{-1}) up to the desired temperature and the spectrum was registered. This procedure was repeated at each temperature.

The specific surface area (BET method) and porosity measurements were performed in a model ASAP 2020 Micromeritics apparatus on 0.30 g of sample, which was heated under vacuum at 473 K for 1 h before the nitrogen adsorption. Temperature programmed reduction experiments were carried out in a model TPD/TPR 2900 Micromeritics equipment. Samples were reduced at a rate of 10 °C min^{-1}, under flow of a 5% H_2/N_2 mixture, at a temperature range of 303–873 K.

Temperature programmed desorption (TPD) of ammonia analyses were carried out in the same equipment. First the sample (0.05 g) was heated at 573 K under helium flow in order to eliminate impurities. Then, it was cooled to 348 K and then pulses of known quantities of ammonia were injected until the complete saturation of the sample. The system was heated up to 1048 K and the TPD profile was obtained. The acidity values were determined from the adsorption peak areas, taking the last peak for calibration.

The metal dispersion was measured by hydrogen chemisorption using a model ASAP 2020 Micromeritics apparatus on 0.25 g of sample, which was previously reduced at 773 K for 2 h under hydrogen flow. The hydrogen chemisorbed was measured by taking an isotherm at 373 K. In order to obtain an independent measurement of the metal dispersion, the cyclohexane dehydrogenation was also performed. It is well known [26–28] that no demanding reactions are useful for characterizing catalysts including the calculation of metal dispersion, when one have standards for calibration [28,29]. The experiments were carried out at atmospheric pressure and 623 K on 0.1 g of sample. The cyclohexane was fed to the microreactor in a hydrogen stream (50 mL min^{-1}) coming from a saturator kept at 293 K. The dispersion values were calculated by comparing the cyclohexane conversion on the samples with the value showed by a known sample (Pt/Al_2O_3).

The XPS spectra were acquired through a VG Scientific spectrometer, Escalab model 220i-XL, with source of X-rays, MgKα (1253 eV) anode and 4000 W power and hemispheric electron analyzer. The Al2p peak (BE = 74.5 eV) was chosen as an internal reference. This reference was in all cases in good agreement with the BE of the C 1s peak, arising from contamination, at 284.6 eV. This reference gives an accuracy of +0.1 eV.

2.3. Catalytic evaluation

Ruthenium-based catalysts were evaluated in methane steam reforming carried out at 923 K and 1 atm with a steam to methane molar ratio of 2. A stainless microreactor, working in a differential

Table 1
Specific surface areas (Sg) of the aluminum (A) and magnesium (M)-based supports (A, M, MA5, MA05, MA02) and of the ruthenium-based catalysts (1% Ru). The numbers represent the magnesium to aluminum molar ratios.

Sample	Sg ($m^2\ g^{-1}$)	Sample	Sg ($m^2\ g^{-1}$)
A	254	RA	242
M	19	RM	14
MA02	218	RMA02	210
MA05	182	RMA05	139
MA5	93	RMA5	24

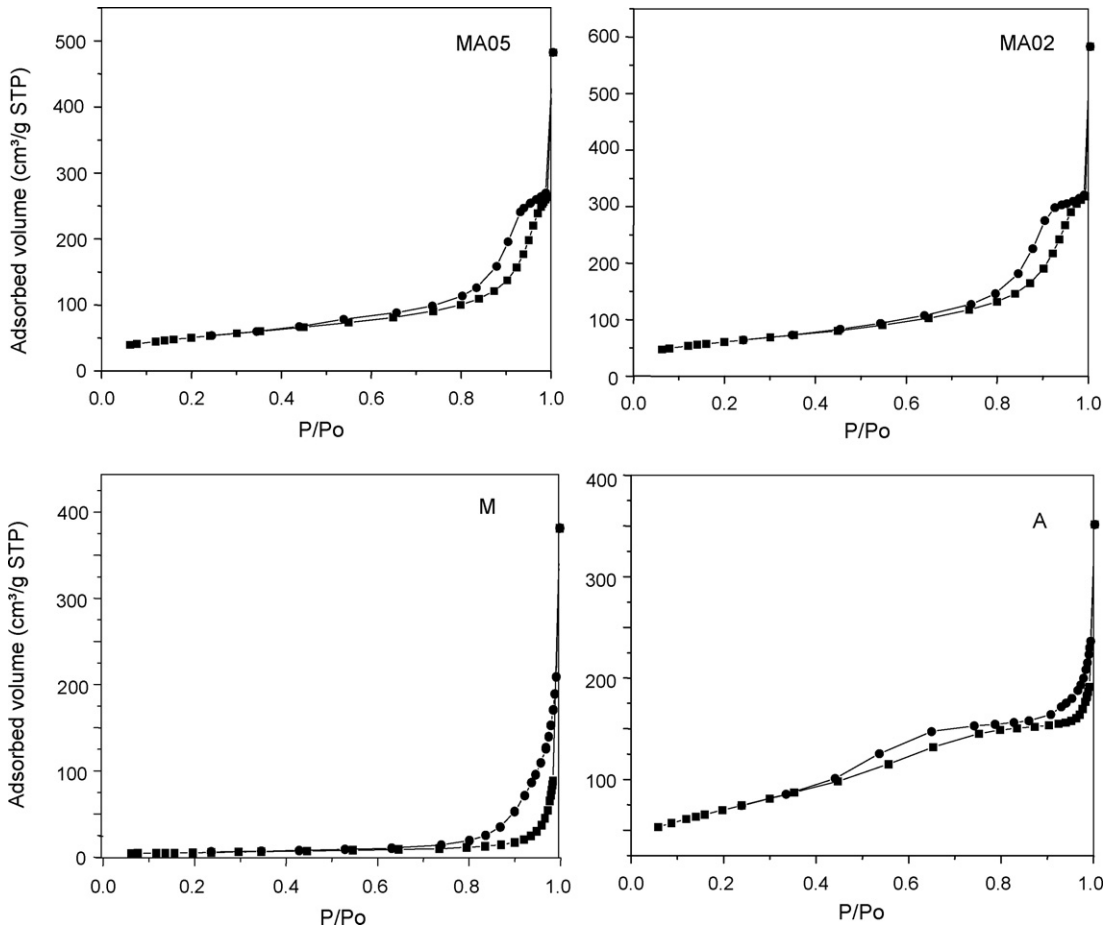

Fig. 4. Adsorption and desorption isotherms of nitrogen at 77 K on the supports.

regime and ascendant flow was used in the experiments. The conditions were adjusted in order to obtain 10% conversion over a commercial catalyst and to avoid difusional effects. Before the catalytic tests, the samples (0.15 g) were reduced in situ under hydrogen flow, at 773 K, for 2 h. The run took 6 h and the reaction products (hydrogen, carbon monoxide and carbon dioxide) as well as the reminiscent methane were analyzed by on line gas chromatography, equipped with thermal conductivity detector (TCD), flame ionization detector (FID) and methanator. The steam was not analyzed but rather removed from the stream before it was fed to the chromatograph. Hydrogen (S_{hid}) and carbon monoxide (S_{mon}) selectivities were calculated by considering the hydrogen atoms and carbon atoms balance, by using the Eqs. (5) and (6), respectively, where n_{hid}, n_{mon} and n_{dio} are the mole number of hydrogen, carbon monoxide and carbon dioxide. The methane conversion was determined using the Eq. (7), where X_{met} is the methane conversion and $n_{met\ (in)}$ and $n_{met\ (out)}$ are the methane moles numbers of inlet and outlet, respectively.

$$S_{hid}(\%) = n_{hid(out)} \times 100/[n_{hid(out)} + 2n_{met(out)}] \quad (5)$$

$$S_{mon}(\%) = n_{mon(out)} \times 100/[n_{mon(out)} + n_{dio(out)} + n_{met(out)}] \quad (6)$$

$$X_{met}(\%) = [n_{met(in)} - n_{met(out)}] \times 100/n_{met(in)} \quad (7)$$

The carbon content of the spent catalysts was determined using 0.05 g of sample and a model 200 CS LECO equipment with induction furnace.

3. Results and discussion

The X-ray diffractograms of aluminum oxide as well as of aluminum and magnesium oxides with molar ratios Mg/Al = 0.2 and 0.5 (Fig. 1a) were very similar showing broad peaks, indicating the formation of poorly crystallized solids and/or solids with small size particles. On the other hand, the magnesium oxide sample showed a profile characteristic of a crystalline solid (Fig. 1b). The identified phase for aluminum oxide was gama-alumina, while the magnesium oxide appeared as periclase, in agreement with the results obtained by other authors [30]. The X-ray profile of aluminum and magnesium oxide with Mg/Al = 5 was similar to that of the pure magnesium oxide (Fig. 1b). These results showed that the addition of low amounts of magnesium (Mg/Al = 0.2 and 0.5) to alumina did not cause a phase change and the gama-alumina structure was preserved; on the other hand, higher amounts of magnesium led to the production of aluminum-containing periclase. The addition of ruthenium to the solids did not change the X-ray patterns, as shown in Fig. 2. No ruthenium phase was detected probably due its low concentration in solids.

The X-ray diffractograms taken at different temperature after heating in situ are shown in Fig. 3. It can be seen that the periclase phase was kept up to 1123 K in the magnesium-richest sample (Mg/Al = 5) while aluminum oxide (γ-Al_2O_3) was more crystallized as the temperature was increased.

Aluminum oxide showed the highest specific surface area (254 $m^2\ g^{-1}$) while magnesium oxide presented the lowest value (19 $m^2\ g^{-1}$), as it can be observed in Table 1. For the solid with the lowest amount of magnesium (MA02 sample), the specific

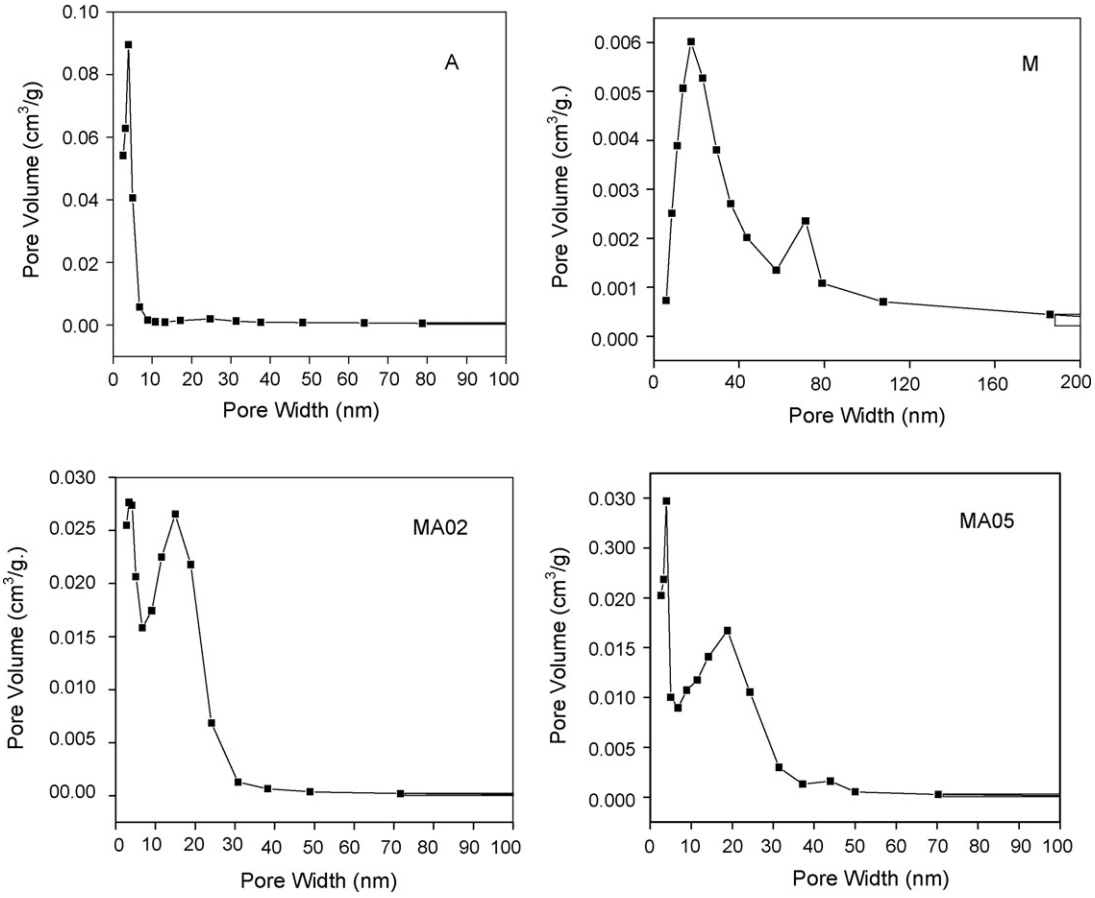

Fig. 5. Pore size distribution curves of the supports.

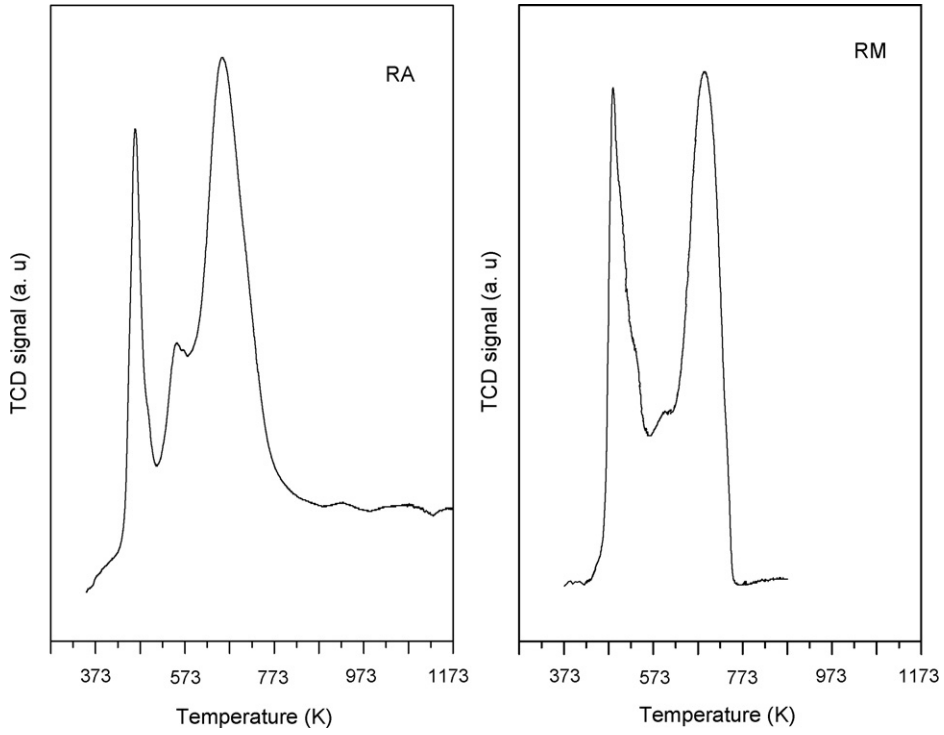

Fig. 6. TPR profiles of alumina-supported ruthenium (RA sample) and of magnesia-supported ruthenium (RM sample).

surface area was close to alumina. However, the specific surface area decreased with the increase of magnesium amount and tended to achieve the value of pure magnesium oxide. This can be related to the change of structure from alumina to periclase as the amount of magnesium increased in the solids, as inferred by X-ray diffraction.

The adsorption and desorption isotherms of nitrogen on the samples and the pore size distribution are shown in Figs. 4 and 5. It can be noted that magnesia has a profile of a Type IV isotherm which is typical of mesoporous solids; the pore size distribution was bimodal in the range of 20 and 70 nm. Alumina showed an isotherm with a similar profile but with domain of mesopororesaround 6 nm (Fig. 5). The addition of magnesium to alumina caused a shift of the hysteresis loop to higher values of relative pressures, indicating that the volume of mesopores increased. The pore distribution curves shows that magnesium changed the curve profile, which became similar to that of magnesia, however, shifted to smaller sizes. This can explain the decrease in specific surface areas due to magnesium.

After ruthenium impregnation, the specific surface area decreased as shown in Table 1. As the temperature used in the calcination of the solid, before and after metal impregnation was the same, this decrease is probably related to the role of ruthenium in promoting the sintering of the particles. In fact, the adsorption and desorption isotherms of nitrogen on the samples before and after impregnation showed the same profile, indicating that the porosity of the samples was not affected by the impregnation process. As expected, the lowest specific surface area was shown by the sample richest in magnesium (RM).

These data can be correlated with the ruthenium dispersions, obtained by different methods, shown in Table 2. As one can

Table 2
Cyclohexane conversion values (X_{CH} %) and metallic dispersion values determined by cyclohexane dehydrogenation reaction (D_{CH} %) and by hydrogen chemisorption (D_{QH} %) for the catalysts. RA and RM samples: alumina-supported ruthenium and magnesia-supported ruthenium; RMA02, RMA05 and RMA5 samples: with Mg/Al (molar) = 0.2, 0.5 and 5 respectively.

Sample	X_{CH} %	D_{CH} %	D_{QH} %
RA	8.0	4.2	9.4
RM	9.4	5.0	–
RMA02	26.0	13.8	44.9
RMA05	24.0	12.7	34.7
RMA5	8.9	4.7	4.6

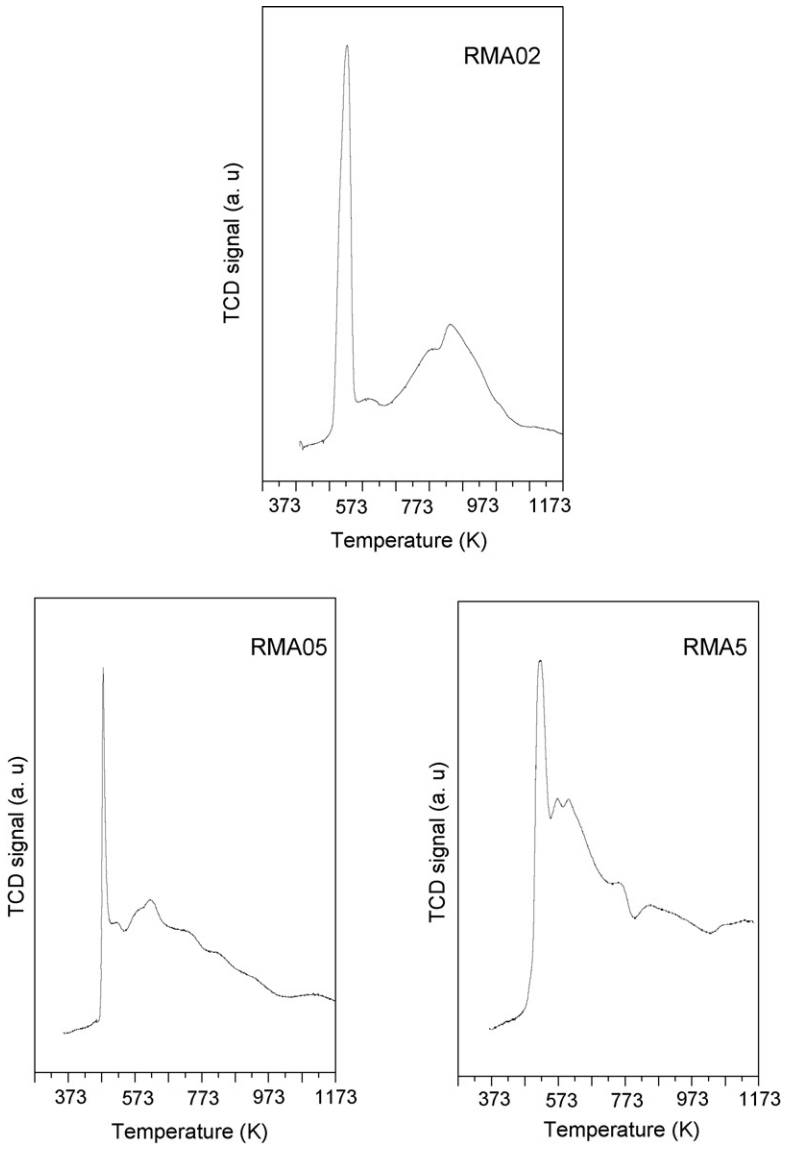

Fig. 7. TPR profiles of the catalysts with magnesium to aluminum molar ratio of 0.2 (RMA02 sample), 0.5 (RMA05) and of 5 (RMA5 sample) and with 1% Ru.

see, magnesia and alumina have quite different specific surface areas, but similar ruthenium dispersions. It suggests that most of ruthenium species is present in the mesopores, which are in smaller amounts in alumina; on the other hand, the addition of magnesium to alumina caused the production of mesopores in the range of 10 and 20 nm, thus increasing the dispersion.

The TPR curves of the catalysts are shown in Figs. 6 and 7. For alumina-supported ruthenium (Fig. 6), one can see two peaks at 473 and 673 K. According to previous work [31] the reduction of Ru^{4+} (RuO_2) to Ru^0 species in alumina-supported ruthenium catalysts occurs in the range of 450–478 K. Other authors [32] found peaks at around 430 K and 470 K, which were assigned to the reduction of ruthenium oxychloride and ruthenium oxide, respectively. In addition, Betancourt et al. [33], based on XPS and hydrogen chemisorption results, assigned the peaks at 463 K and 496 K to a well-dispersed ruthenium phase and to the reduction of RuO_2 compound, respectively. On the other hand, the high temperature peak can be assigned to the reduction of strongly interacted RuO_2 species formed at the interface between the metal and the support, as previously reported [34,35]. In magnesia-supported ruthenium, these peaks appeared in the same temperature range. The addition of magnesium to the alumina-supported ruthenium caused an increase of the interactions between ruthenium species and the support, as we can infer by the shift of first peak to higher temperatures for the RMA02 sample (512 K), the RMA05 sample (477 K) and the RMA5 sample (489 K) as compared to alumina-based catalyst. However, no simple relationship was found between these variables, probably due to the different magnesium distribution in solids as well as to the phase change from alumina to periclase. In all cases, the high temperature peak is broad due to reducible species in the support.

The TPD curves of selected samples are shown in Fig. 8, while the total acidity and the acidic sites, calculated from these curves, are displayed in Table 3. In the calculation of the acidic sites of the samples, the sites with weak acidity were considered as those whose desorption temperature was in the range of 366–555 K while the sites of moderate acidity were those in the range of 622–764 K. The strong acidity sites were those which desorbed ammonia in the range of 800–954 K. As expected, the addition of magnesium to alumina caused a decrease in acidity, as found by other authors [19,36]. It can also be noted, from Table 3, that this decrease occurs mainly as the expenses of a loss of strong acidic sites and a few weak acidic sites, while the moderate acidic sites were not affected by magnesium.

The binding energies (BE) of Ru $3d_{5/2}$ and Mg 2p core-levels of the samples are compiled in Table 4. Fig. 9 illustrates typical XPS spectra. All samples showed binding energies characteristic of and Ru^{4+} species in ruthenium oxide (RuO_2) [37] but the values differ slightly, indicating the presence of species in different electronic states. It can be noted that the addition of small amounts of magnesium (Al/Mg = 0.2) to alumina-supported ruthenium (RMA02 sample) led to the formation of electron deficient ruthenium species, while higher amounts did not change the electronic properties of ruthenium. The BE energy of magnesium (48.6 eV) is typical of Mg^{2+} species [37]. The amount of ruthenium and magnesium was higher on the surface for the magnesium-richest sample (RMA5 sample).

The methane conversion and the hydrogen to carbon monoxide molar ratio, calculated according Maluf et al [38], as well as the amount of coke are shown in Table 5. All samples showed conversions close or higher than a commercial nickel-based catalyst (10%). The values for the catalysts based on pure oxides (alumina and magnesia) largely differed from each other and the magnesia-supported ruthenium led to the highest conversion. The aluminum and magnesium-oxides supported ruthenium led to similar conversion values which are close to that of the alumina-based catalyst. However, the hydrogen to carbon monoxide molar ratios were quite different for the catalysts. It can be assigned to the different abilities of the catalysts in promoting the water gas shift reaction. This is an important finding since it allows tailoring the catalysts to different applications. The sample with the lowest

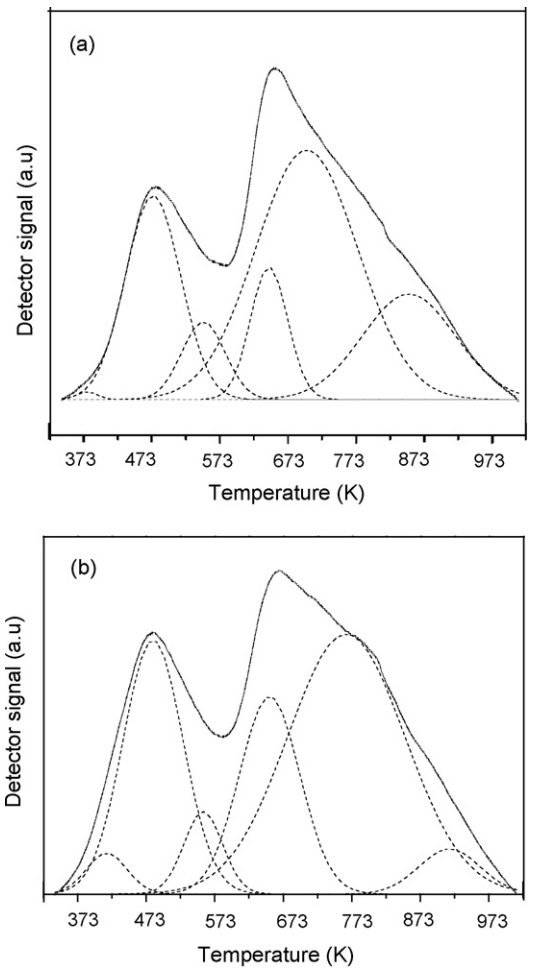

Fig. 8. TPD curves of the ruthenium (1%) catalysts supported (a) on alumina (RA) and (b) on aluminum and magnesium-based support with Mg/Al = 0.5 (RMA05).

Table 3
Total acidity and acidic site distribution for alumina-supported ruthenium (RA) and for the catalyst with magnesium to aluminum molar ratio (RMA05).

Sample	Acidic site concentration (μmol NH_3 ads g^{-1})	Acidic site distribution[a] (μmol de NH_3 ads g^{-1})		
		366–555 K (weak)	622–764 K (moderate)	799–954 K (strong)
RA	40.1	10.8 (27%)	22.2 (55%)	7.1 (18%)
RMA05	31.9	8.7 (28%)	21.8 (68%)	1.4 (4%)

[a] Calculated from the TPD curves.

Table 4
Binding energies (eV) of core-levels and surface composition of alumina-supported ruthenium (RA sample) and aluminum (a) and magnesium-supported ruthenium with Mg/Al = 0.2 (RMA02 sample) and 5 (RAM5 sample).

Sample	Ru 3d (eV)	Ru 3d (at. %)	Mg/Al	Ru/(Al + Mg)
RA	282.1	0.445	–	0.005
RMA02	281.5	0.252	0.137	0.0034
RMA5	282.6	0.164	0.368	0.0139

Table 5
Methane conversion (X_{met}), hydrogen to carbon monoxide ratio (H_2/CO) and coke deposited during reaction (C) for the catalysts in methane steam reforming. RA and RM samples: alumina-supported ruthenium and magnesia-supported ruthenium; RMA02, RMA05 and RMA5 samples: with Mg/Al (molar) = 0.2, 0.5 and 5, respectively.

Sample	X_{met} (%)	H_2/CO	C (%)
RA	10	25	0.24
RM	28	18	0.53
RMA02	10	6	0.34
RMA05	6.9	20	0.37
RMA5	7.6	32	0.75

amount of magnesium (RMA02) showed the lowest ratio, a fact which can be related to the presence of electron deficient ruthenium species (as detected by XPS), which are less active for water gas shift reaction (Fig. 9).

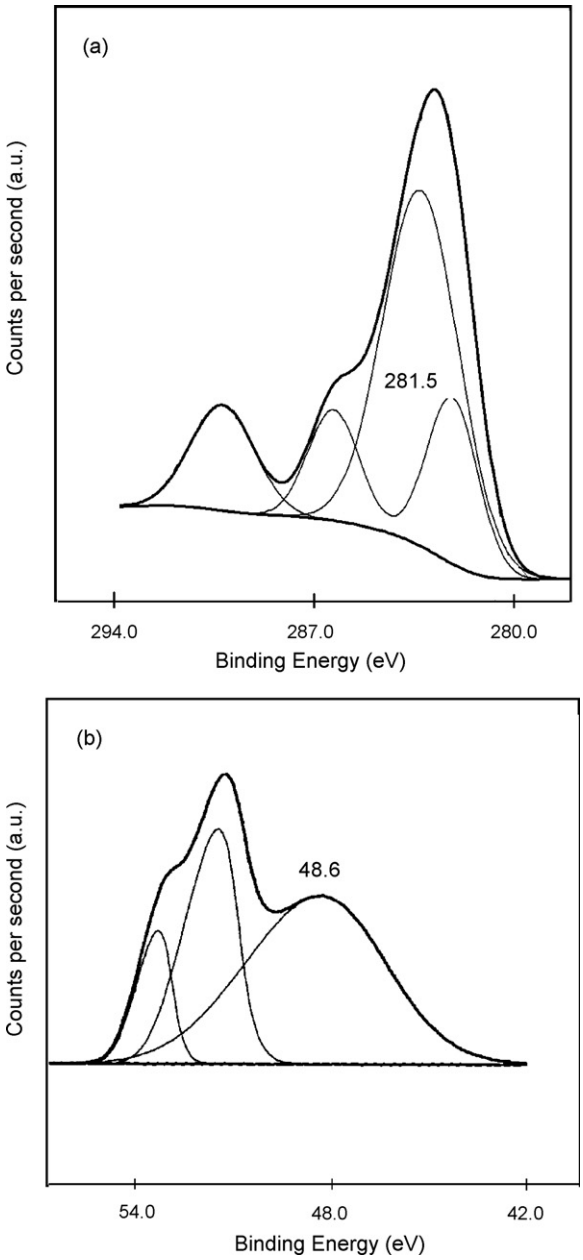

Fig. 9. Core-level spectra of (a) Ru 3d for alumina-supported ruthenium (RA sample) and of (b) Mg 2p for the aluminum and magnesium oxides-supported ruthenium with Mg/Al = 0.2 (AM02 sample).

All catalysts presented very low selectivity to carbon monoxide, indicating that ruthenium-based catalysts can be a promising alternative to get pure high hydrogen, with low carbon monoxide content. This is particularly interesting for application in fuel cells, in which the amount of carbon monoxide in hydrogen stream must remain very low, since it is a strong poison for the electrodes [39]. In the operation conditions used in this work, the water gas shift reaction also occurs and seems be promoted in a large extension by the studied catalysts.

These results cannot be explained by the amount of ruthenium species exposed on the surface, as we can see by comparing Tables 2–5. As we can see, both from the dispersion measurements and the cyclohexane dehydrogenation (Table 2), as well as from the XPS results (Table 4), the catalysts with low amounts of magnesium (RMA02 and RM05 samples) showed the highest dispersions but led to low methane conversions (Table 5). The dispersion values for the other catalysts cannot be correlated to methane conversion either. It means that the support is playing a role in determining the catalytic activity, in accordance with other works [40].

In fact, several authors [17,41] pointed out that the steam reforming reaction takes place at the metal-support interface, through the reaction between the water preferentially adsorbed on the support, which is formulated to allow the mobility of oxygen species originated from water dissociation on the surface and the methane preferentially adsorbed on the metal. Also, by increasing water adsorption-dissociation rate on the catalyst coke production is prevented [42]. In addition, it is well known [40] that alkaline earth oxides, such as magnesium oxide, calcium oxide and barium oxide are often incorporated into steam reforming catalysts to provide operational advantages resulting from lower support acidity, higher metal dispersions and improved steam activation. Besides, as pointed out earlier [43] the support acidic sites consume ruthenium electrons and then the high acidity of the support has a detrimental effect on the activity. The results obtained in the present work showed that the addition of magnesium in the range of Mg/Al = 0.2–5 is not enough to increase the activity in methane conversion, suggesting that the water adsorption-dissociation was not improved by magnesium.

However, the addition of different amounts of magnesium affects the activity of the catalysts to water gas shift reaction and this allows getting different hydrogen to carbon molar ratios.

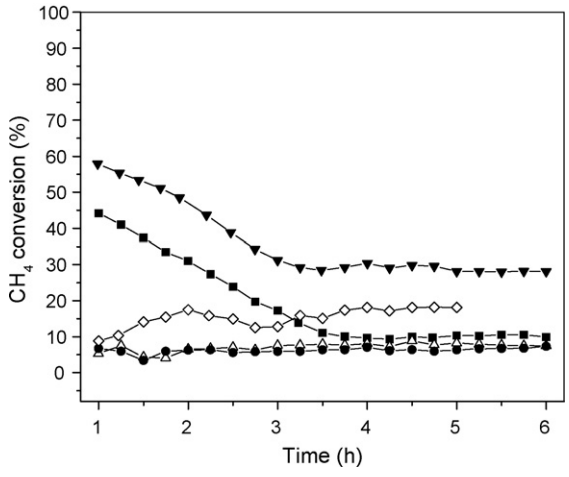

Fig. 10. Methane conversion as a function of time reaction in steam reforming on the catalysts. RA (■) and RM (▼) samples: alumina-supported ruthenium and magnesia-supported ruthenium; RMA02, RMA05 and RMA5 samples: with Mg/Al (molar) = 0.2 (◇), 0.5 (●) and 5 (△) respectively.

Fig. 10 shows the methane conversion as a function of time for the catalysts. It can be noted that alumina-supported ruthenium and magnesia-supported ruthenium showed deactivation in the first 3 h, while the other catalysts were stable since the beginning of reaction. Therefore, the supports based on aluminum and magnesium have the advantage of increasing the stability of the catalyst. However, this deactivation has no simple relationship with coke deposition as we can see in Table 5. In all cases, the coke was very low, as expected due to the well known effect of the noble metals in preventing coke deposition [20].

4. Conclusions

The addition of small amounts of magnesium to alumina-supported ruthenium (Mg/Al (molar) = 0.2–0.5) does not change the gama-alumina structure but high amounts (Mg/Al (molar) = 5) lead to the production of periclase. Magnesium causes a decrease of specific surface area of the catalysts and this effect increases with its amount in solids. The interaction between ruthenium and the support increases due to magnesium but there is no simple relationship between this effect and the amount of the metal. As expected, magnesium decreases the acidity of alumina-supported ruthenium and generates electron deficient ruthenium species. The addition of magnesium also increases the ruthenium dispersion but does not increase the methane conversion. It means that the acidity of support plays a role in affecting the ruthenium activity in methane conversion. Magnesium is also able to change the catalytic activity of the samples towards the water gas shift reaction, allowing the tailoring of the hydrogen to carbon monoxide molar ratio. The catalysts show activity close or higher than a commercial sample, indicating that they are promising for the reaction. The methodology used in this work has been proved to be useful for tailoring ruthenium-based catalysts for several applications.

Acknowledgments

L.S.C. and A.R.M. acknowledge FAPESB and CNPq for the scholarships. The authors acknowledge CNPq and FINEP for the financial support.

References

[1] C. Pistonesi, A. Juan, B. Irigoyen, N. Amadeo, Appl. Surf. Sci. 253 (2007) 4427.
[2] M.A. Peña, J.P. Gómez, J.L.G. Fierro, Appl. Catal. A: Gen. 144 (1996) 7.
[3] M.E. Dry, in: J.R. Anderson, M. Boudart (Eds.), Catalysis: Science and Technology, vol. 1, Springer-Verlag, New York, 1984, p. 106.
[4] S.C. Tsang, J.B. Claridge, M.L.H. Green, Catal. Today 23 (1995) 3.
[5] L.C.P. Fernandes Júnior, S. de Miguel, J.L.G. Fierro, M.C. Rangel, Stud. Surf. Sci. Catal. 167 (2007) 499.
[6] G.C. Araujo, S.M. Lima, J.M. Assaf, M.A. Pena, J.L.G. Fierro, M.C. Rangel, Catal. Today 133–135 (2008) 129.
[7] J.R.H. Cross, A.N.J. van Keulen, M.E.S. Hegarty, K. Seshan, Catal. Today 30 (1996) 193.
[8] J.R. Rostrum-Nielsen, Catal. Today 18 (1993) 305.
[9] M.V. Twigg, Catalyst Handbook, 2nd ed., Wolfe Publishing Ltd., London, 1989.
[10] A.V. Silva Neto, P.P.C. Sartoratto, M.C. Rangel, Stud. Surf. Sci. Catal. 167 (2007) 475.
[11] M.A. El-Bousiffi, D.J. Gunn, Int. J. Heat Mass Transfer 50 (2007) 723–733.
[12] H.-S. Roh, K.-W. Jun, W.-S. Dong, J.-S. Chang, S.-E. Park, Y.-I. Joe, J. Mol. Catal. 181 (2002) 137.
[13] S.P. Lima, V. Vicentini, J.L.G. Fierro, M.C. Rangel, Catal. Today 133–135 (2008) 925.
[14] A. Berman, R.K. Karn, M. Epstein, Appl. Catal. 282 (2005) 73.
[15] T. Caillot, P. Gélin, J. Dailly, G. Gouthier, C. Cayron, J. Laurencin, Catal. Today 128 (2007) 264.
[16] D.L. Trimm, Catal. Today 49 (1999) 3.
[17] J.R. Rostrup Nielsen, J. Schested, Adv. Catal. 47 (2002) 65.
[18] F. Melo, N. Morlanés, Catal. Today 107 (2005) 458.
[19] M. Kumar, F. Aberuagba, J.K. Gupta, K.S. Rawat, L.D. Sharma, G. Murali Dhar, J. Mol. Catal. 213 (2004) 217.
[20] H. Al-Qahtani, Chem. Eng. J. 66 (1997) 51.
[21] Y. Ono, T. Baba, Catal. Today 38 (1997) 321.
[22] M. Ziolek, J. Kujawa, J. Czyzniewska, I. Nowak, A. Aboulayt, O. Saur, J.C. Lavalley, Appl. Catal. A 171 (1998) 109.
[23] T. Horiuchi, H. Hidaka, T. Fukui, Y. Kubo, M. Horio, K. Suzuki, T. Mori, Appl. Catal. A 167 (1998) 195.
[24] L. Kiwi-Minsker, G. Jenzer, L. Pliasova, A. Renken, Stud. Surf. Sci. Catal. 121 (1999) 159.
[25] S. Golay, L. Kiwi-Minsker, R. Doepper, A. Renken, Chem. Eng. Sci. 54 (1999) 3593.
[26] P. Pantu, G. Gavalas, Appl. Catal. A 223 (2002) 253.
[27] C. Carnevillier, F. Epron, P. Marecot, Appl. Catal. A 275 (2004) 25.
[28] E. Rogemond, N. Essayeng, R. Fréty, V. Perrichon, M. Primet, F. Mathis, J. Catal. 166 (1997) 229.
[29] C. Pieck, C.R. Vera, J.M. Parera, G.N. Giménez, L.R. Serra, L.S. Carvalho, M.C. Rangel, Catal. Today 107–108 (2005) 637.
[30] J. Guo, H. Lou, H. Zhao, X. Wang, X. Zheng, Mater. Lett. 58 (2004) 1920.
[31] P.G.J. Koopman, A.P.J. Kieboom, H. van Bekkum, J. Catal. 69 (1981) 172.
[32] V. Mazzieri, F. Coloma-Pascual, A. Arcoya, P.C. L'Argentière, N.S. Fígoli, Appl. Surf. Sci. 210 (2003) 222.
[33] P. Betancourt, A. Rives, R. Hubaut, C.E. Scout, J. Goldwasser, Appl. Catal. A 170 (1998) 307.
[34] D. Li, N. Ichikuni, S. Shimazu, T. Uematsu, Appl. Catal. A 172 (1998) 351.
[35] P.S.S. Reddy, N. Pasha, M.G.V.C. Rao, N. Lingaiah, I. Suryanarayana, P.S.S. Prasad, Catal. Commun. 8 (2007) 1406.
[36] F. Aberuagba, M. Kumar, J.K. Gupta, G. Murali Dhar, L.D. Sharma, React. Kinet. Catal. Lett. 75 (2002) 245.
[37] C.D. Wagner, W.M. Riggs, L.E. Davis, J.F. Moulder, G.E. Muilenberg, Handbook of X-Ray Photoelectron Spectroscopy, PerkinElmer Coorporation, Eden Prairie, 1978, pp. 48, 106.
[38] S.S. Maluf, E.M. Assaf, J.M. Assaf, Quím. Nova 26 (2003) 181.
[39] L. Villegas, N. Guillaume, H. Provendier, C. Daniel, F. Masset, C. Mirodatos, Appl. Catal. A 281 (2005) 75.
[40] J.T. Richardson, B. Turk, M.V. Twigg, Appl. Catal. A: Gen. 148 (1996) 97.
[41] F. Melo, N. Morlanés, Catal. Today 133–135 (2008) 383.
[42] J. Zhang, Y. Wang, R. Ma, D. Wu, Appl. Catal. A:Gen. 243 (2003) 251.
[43] Y. Kadowaki, K. Aika, J. Catal. 161 (1996) 178.